Available online at www.sciencedirect.com
ScienceDirect
Journal of the European Ceramic Society 26 (2006) 3881–3886
www.elsevier.com/locate/jeurceramsoc

Wetting behaviour of Y_2O_3/AlN additive on SiC ceramics

R.M. Balestra *, S. Ribeiro, S.P. Taguchi, F.V. Motta, C. Bormio-Nunes

Department of Materials Engineering (DEMAR), Faculty of Chemical Engineering of Lorena (FAENQUIL), Polo Urbo Industrial, Gleba AI6, CP 116, 12600-970 Lorena, SP, Brazil

Received 2 May 2005; received in revised form 27 November 2005; accepted 16 December 2005
Available online 20 February 2006

Abstract

The wetting of SiC plate by Y_2O_3/AlN additive was analysed using the sessile drop method. The wetting behaviour was observed by image capture system using a CCD camera during the heating, in argon atmosphere. The contact angle was measured as a function of temperature and time. After the wetting test the SiC plus additive samples were cut in order to observe the thickness plate cross section. The additive area and the interface between SiC and additive were analysed using scanning electron microscopy (SEM) and energy dispersive spectrometry (EDS). The wetting of SiC by Y_2O_3/AlN is influenced by the presence of a solid phase in some of the additive drops that depends mainly on the additive composition and consequently on the temperature. The measured contact angles were below 7°, reaching 0° for Y_2O_3/AlN additive tested at the eutectic composition, indicating a very good wettability of Y_2O_3/AlN on the SiC.

Keywords: Wettability; Interfaces; SiC; Y_2O_3; AlN

1. Introduction

It is well known that the bonds between silicon and carbon atoms in SiC (silicon carbide) are very strong, as a consequence, SiC has a low self-diffusion coefficient. This property limits the production of high density SiC ceramics by solid phase sintering. In order to get a high density ceramic, some metallic oxides (additives) can be added to SiC. The objective is to form a liquid phase during the sintering. The liquid phase sintering (LPS) results in a material with an homogeneous microstructure and therefore suitable to achieve good mechanical properties such as a high toughness.[1–6]

The important variable of the LPS process to obtain SiC ceramic is the wetting of the solid phase (SiC) by the liquid phase (additive). The wetting behaviour is measured through the contact angle (θ) between the solid SiC and the liquid drop formed by the additive. The solid–liquid systems may be of two types, i.e. non-reactive and reactive. In non-reactive systems, the contact angle θ is expressed as a function of the surface energies solid–liquid (γ^{SL}), liquid–vapour (γ^{LV}), solid–vapour (γ^{SV}), as well as the adhesion work (W_a). The mutual dependence of surface energies, adhesion work and contact angle is described by Young and Yong-Dupré equations,[7–16] that are given by Eqs. (1) and (2):

$$\gamma^{SV} = \gamma^{SL} + \gamma^{LV}\cos\theta \tag{1}$$

$$W_a = \gamma^{LV}(1 + \cos\theta) \tag{2}$$

When a reaction occurs at the interface, the free energy change per unit area per unit time also enhances wetting. In this case, the Young equation should be corrected for this driving force.[7,10] The smallest contact angle in reactive system is given by Eq. (3),

$$\cos\theta_{min} = \cos\theta_0 - \frac{\Delta\gamma_r}{\gamma_{LV}} - \frac{\Delta G_r}{\gamma_{LV}} \tag{3}$$

where θ_0 is the contact angle of the liquid on the substrate in the absence of any reaction, ΔG_r is the Gibbs free energy of the chemical reaction, γ_r is the change in the interfacial energies brought about by the chemical reaction.

One possible source of reaction is related to the oxygen partial pressure in the furnace. The reaction of oxygen with the substrate of SiC can form a thin film of SiO_2. However, at temperatures higher than 1475 K, in vacuum, the SiO_2 film evaporates according to the reaction of Eq. (4).[10]

$$2\langle SiO_2\rangle_s + \langle SiC\rangle_s \rightarrow 3(SiO)_g \uparrow + (CO)_g \uparrow \tag{4}$$

* Corresponding author. Tel.: +55 012 3159 9954; fax: +55 012 3153 3006.
E-mail address: roselibalestra@yahoo.com.br (R.M. Balestra).

0955-2219/$ – see front matter © 2006 Elsevier Ltd. All rights reserved.
doi:10.1016/j.jeurceramsoc.2005.12.022

Under these conditions a pure SiC surface is formed and it is more realistic for this system than the measurement at lower temperatures.

The reaction of the oxygen with the additives is very important in metal/ceramic oxides. Usually a thick oxide film forms on the sessile drop and oxidation is evident because the surface of the liquid is not smooth at melting.[17,18] However, in oxide additive the oxygen is already part of the composition and an appreciable effect on interfacial energies are not expected. The furnace atmosphere can also modify the viscosities of the melt. The melt viscosity can change with composition of the melt and with temperature, as shown in the literature.[10,14–16,19]

The usual experimental method used to measure the contact angle is the sessile drop method. In this method, a photography system register the additive sample for increasing temperature in determined time intervals pictures of the drop shape evolution, just before and after the drop starts to melt.[12–14] The contact angle is measured in each picture of a sequence, using a computational program.

Due to the importance of the wettability on the liquid phase sintering, it is the objective of this work to evaluate the wettability of the Y_2O_3/AlN additive on the SiC as a function of the temperature, time and compositions using the sessile drop method.

2. Experimental

The substrates were SiC plates of density 98.9%, sintered via solid state obtained from Wacker – Chemie GmbH, Germany. The substrates had dimensions 10 mm × 10 mm × 4 mm, were ground and polished using diamond suspension down to 1 μm to minimise the surface roughness. SiC plate surfaces were cleaned by acetone and deionised water.

GRADE C powders of Y_2O_3 and AlN from Hermann C. Starck – HCST were used to produce the additives for three different compositions. One of the selected compositions is that of the eutectic point (YN2) and the other two are just at the left (YN1) and at the right side (YN3) of the eutectic one. These compositions are indicated in the Y_2O_3–AlN phase diagram showed in Fig. 1. In order to get the additives samples, Y_2O_3 and AlN powders were mixed using isopropyl alcohol in an attrition milling for 1 h at 1000 rpm. The slurry was dried at 80 °C in a vacuum rotating drier. Green bodies spheres of 4 mm diameter were pressed at 90 MPa using a Monostatic 50 Powder Press – Simac. The molar and mass concentrations of Y_2O_3 and AlN of each additive are presented in Table 1.

Table 1
Compositions of the additives

Additive code	Composition			
	mol%		wt.%	
	Y_2O_3	AlN	Y_2O_3	AlN
YN1	50	50	84.64	15.36
YN2	57	43	87.96	12.04
YN3	60	40	89.21	10.79

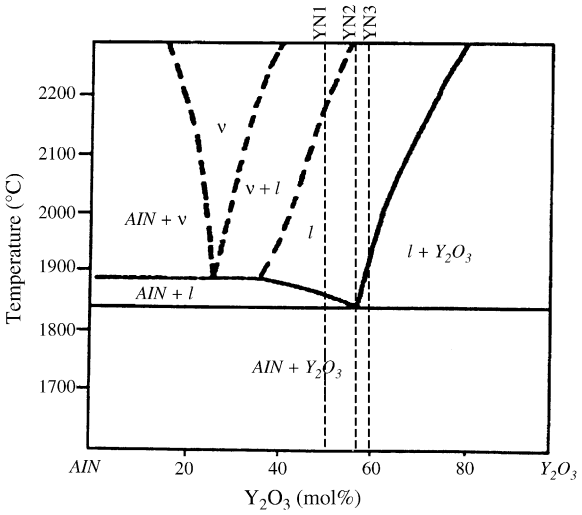

Fig. 1. Phase diagram of the Y_2O_3/AlN system.[3]

The additive spheres were put on the SiC plate and the set was heated up in a graphite furnace of Thermal Technology Inc. (ASTRO) at 10 °C/min, under a pressure of 0.1 MPa of analytical grade argon. Before starting the test, the furnace camera was flushed out with argon to remove the oxygen. In a first experiment, an imaging system capture with a CCD camera (photography system) registers in determined time intervals, pictures of the drop shape evolution for increasing temperature. This test was performed for YN1, YN2 and YN3 additives. While, the experiment at constant temperature (T = 1850 °C) was carried out only for the additive YN2. During the tests, the pictures are taken when visible changes in the spreading of the additive liquid on SiC can be noticed. The contact angle is measured in each picture of a sequence, using a QWin Leica software.

After wetting experiments, images of the interfaces between SiC and additives were taken by SEM/BSE (scanning electron microscopy/back-scattered electrons). The elements present in each phase of the additive region were identified via energy dispersive X-ray analysis (EDS). The EDS measurements and SEM images were carried out in a LEO-Zeiss 1450VP microscope, at 20 kV accelerating voltage.

3. Results and discussion

Fig. 2 shows three rows of images for additive drop shape evolution. Four representative images are shown in each row for YN1 (first row from the top), YN2 (second) and YN3 (third) additives. These images were registered during wetting tests for variable temperature. One test for isothermal conditions (T = 1850 °C) was made for the YN2 additive and the corresponding row of images is shown in Fig. 3. From these images is observable that the surface of the drops is very smooth, indicating that no reaction is occurring between the additive and the furnace atmosphere.

The experimental data of the contact angle θ as a function of temperature T is plotted in Fig. 4 together with the fitting curves for each additive. Experimental results of θ versus T were fitted for temperatures $T \geq T_0$. T_0 corresponds to the eutetic temper-

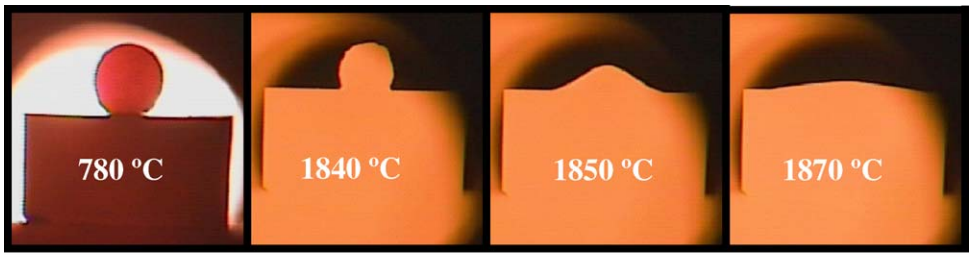

(a)

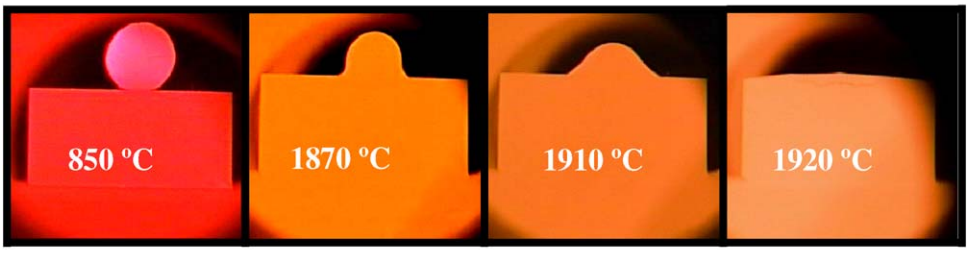

(b)

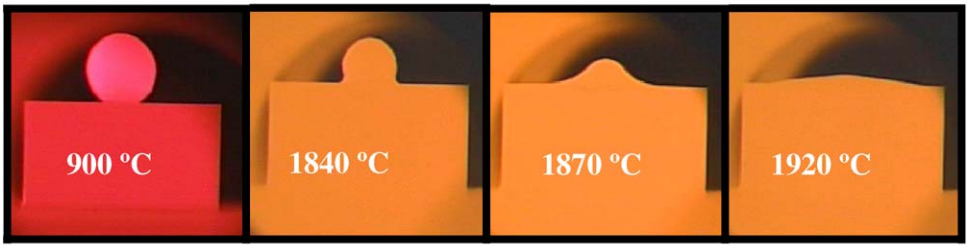

(c)

Fig. 2. Sequential images of the drop shape evolution during wettability tests for: (a) YN1, (b) YN2 and (c) YN3, for increasing the temperatures.

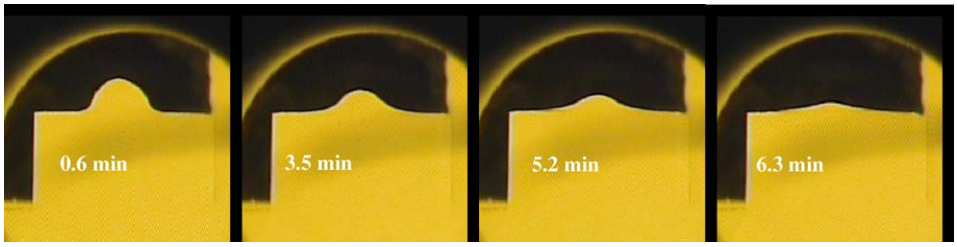

Fig. 3. Sequential images of the drop shape evolution during wettability test for additive YN2 at $T = 1850\,^{\circ}\mathrm{C}$, at minutes indicated on each images.

ature and was determined from the phase diagram (Fig. 1). At $T_0 = 1840\,^{\circ}\mathrm{C}$, the selected additives start to melt. Eqs. (4) and (5) are the formulas obtained from mathematical fitting for additives YN1–YN3 (Eq. (4)) and YN2 (Eq. (5)):

$$\theta_{\mathrm{YN1,YN3}} = \theta_{\min} + \theta_{\mathrm{P}} \exp\left[-\alpha_{\mathrm{D}}(T - T_0)\right] \quad (4)$$

$$\theta_{\mathrm{YN2}} = \theta_{\mathrm{P}} + 0.05(T - T_0) - 0.017(T - T_0)^2 \quad (5)$$

where $\theta_{\min}$ is the minimum contact angle, $(\theta_{\min} + \theta_{\mathrm{P}})$ is the initial contact angle at $T = T_0$ and α_{D} is the exponential decay factor.

In Table 2, the values for $\theta_{\min}$, $(\theta_{\min} + \theta_{\mathrm{i}})$ and α_{D} are presented. Moreover, Table 2 shows the temperature of the total melting T_{m} for each additive and the phases present in the temperature rang of $T_0 \leq T \leq T_{\mathrm{m}}$, in accordance to the phase diagram.

The θ versus T curves for YN1 and YN3 additives have similar behavior; however, for additive YN2 this behavior is quite different. Additives YN1 and YN3 exhibit an exponential decay of θ with T, though a quadratic decay is shown by YN2 additive. Therefore, in the temperature range between 1840 °C and approximately 1910 °C, θ values for YN2 additive are larger

Table 2
Values of $\theta_{\min}$, α_{D} and T_{m} for YN1, YN2 and YN3 additives

Additive	$\theta_{\min}$ (°)	$(\theta_{\min} + \theta_{\mathrm{P}})$ (°)	α_{D} (°C)$^{-1}$	T_{m} (°C)	Drop phases
YN1	6	68	0.133	1870	Liquid + AlN
YN2	0	105	–	1840	Liquid
YN3	6	60	0.0420	1930	Liquid + Y_2O_3

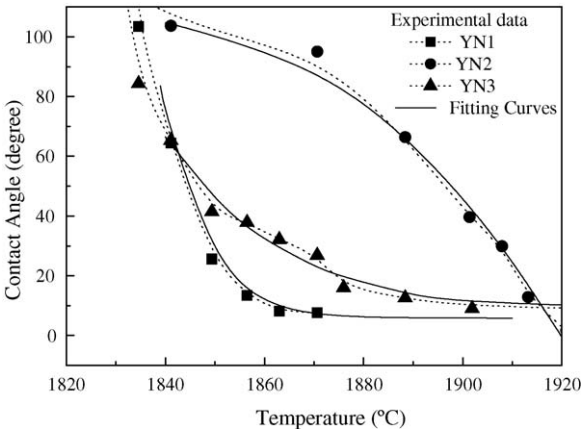

Fig. 4. Contact angle (θ) vs. temperature (T) curves of additives: YN1, YN2 and YN3 on SiC plates.

compared to values for YN1 and YN3 additives because $\theta_{YN2}(T)$ decays slowly than $\theta_{YN1,\,YN3}(T)$.

The stronger decrease of θ with T for YN1 and YN3 was found to be associated to the presence of solid phases in the drop of YN1 and YN3 additives for $T < T_m$ (see Table 2) that causes the decrease of the surface energies γ^{LV} and γ^{SL}. This founding is in accordance with Eq. (1) because the decrease of γ^{LV} and γ^{SL} cause the increase of $\cos\theta$ and therefore the decrease of θ.[16,19] The Eq. (1) was cited because although of the additives react itself, they not react with SiC, characterizing a physical wet.

It was attributed to small differences between additives YN1 and YN3 θ versus T behavior to the distinct solids that are present in each drop, namely, AlN for YN1 and Y_2O_3 for YN3. Although for both additives the minimum contact angle tends to $\theta_{min} \approx 6^\circ$; θ_{min} is reached at $T \approx 1890\,^\circ C$ for additive YN1 and for additive

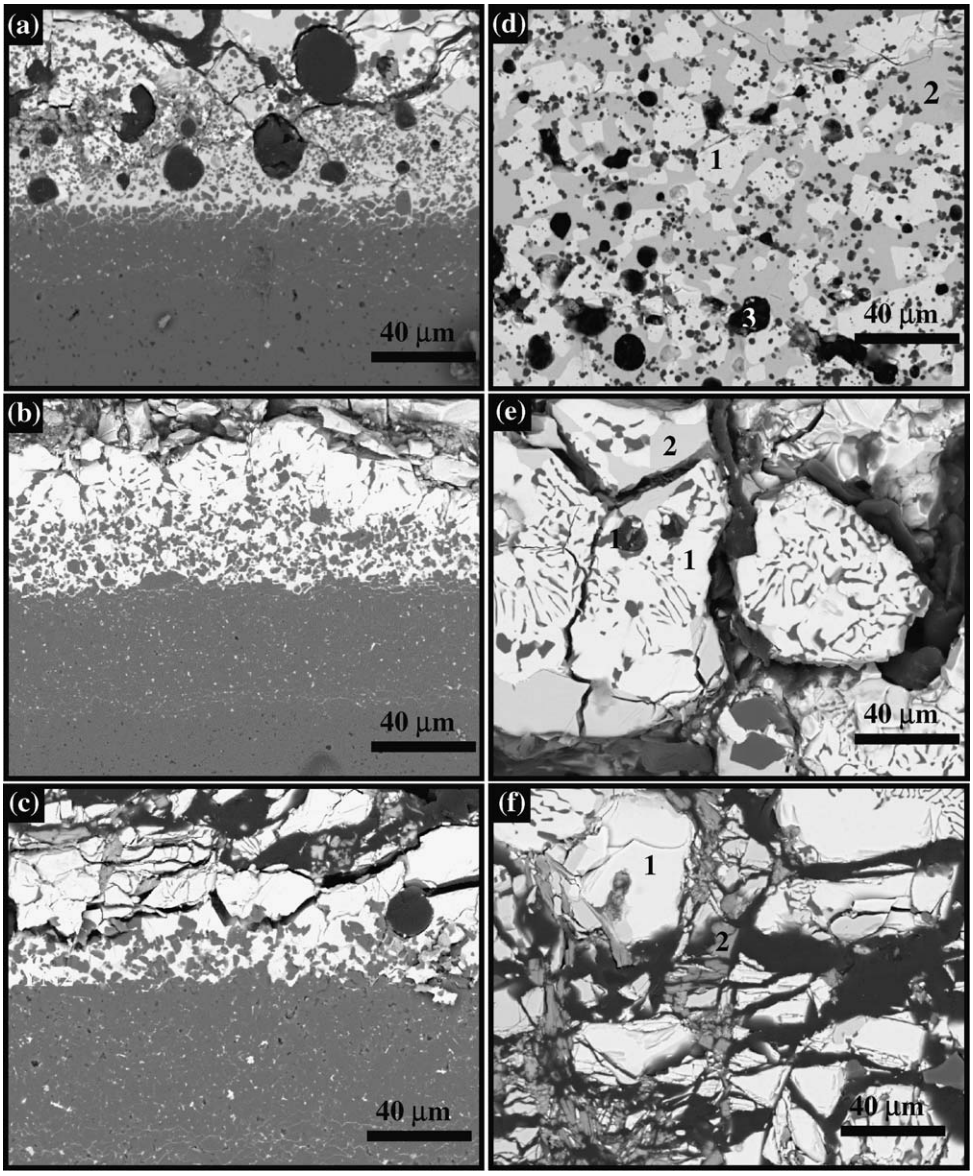

Fig. 5. SEM micrograph of interface between SiC and additive (column at the left side) and magnification of the additive region (column at the right side) respectively for: (a) and (d) YN1; (b) and (e) YN2; (c) and (f) YN3.

YN3 at $T \approx 1990\,^{\circ}C$. These temperatures are about 1–3% above T_m, the temperature of complete melting, in each case.

The values of minimum contact angles for YN1 and YN3 additives are rather small, revealing a good wettability, however the complete wettability $\theta_{min} \approx 0^{\circ}$, could not be reached.

In Fig. 5, micrographs of the interfaces between SiC substrate and additives YN1, YN2 and YN3 are shown in the column at the left side and the amplified regions of the additives in the column at the right side. For the three additives, the presence of SiC particles was detected at the interface, suggesting a partial dissolution of the solid SiC. The amount of SiC particles is much higher for YN2 than for YN1 and YN3 additives. As a result, a thicker layer of additive YN2 plus SiC is produced compared to YN1 and YN3 additives. In the case of additive YN2, the contact of the solid occurs with a larger quantity of liquid, since the onset of the experiment. Then, the wettability improvement of YN2 additive is related to a better dissolution that causes a significant modification of the initial characteristics of the solid surface.[16,17] In the case of additives YN1 e YN3 there is probably the competition of the spreading with the dissolution.

The microstructures of the additives YN2 and YN3 showed in Fig. 5 (column at the right side) are similar. However, the additive YN1 microstructure presents smaller grain sizes compared to YN2 and YN3. For all additives, EDS measurements in the lightest gray region (#1) revealed the presence of Y and O and in the darker gray region (#2) the elements present are O, Y and Al. Only the microstructure of the additive YN1 presents presented a third phase (#3) that is black and the elements identified in this phase are Al and N. Most likely, phase #1 is pure Y_2O_3, phase #2 is a solid solution of Y_2O_3 + AlN and phase #3 is pure AlN.

Both YN2 and YN3 additives microstructure present a lamellar structure that is a characteristic of a eutectic composition. In YN3 sample the eutectic structure fraction is smaller than in YN2 sample, as expected.

Fig. 6 shows the curve of the contact angle as a function of time (t) for additive YN2 at $T = 1850\,^{\circ}C$. Eq. (6) is the formula obtained by fitting the experimental data and shows an exponential decay of θ_{YN2} versus t.

$$\theta_{YN2}(t) = 66.2 \exp(-\alpha_D t) \quad (6)$$

with $\alpha_D = 0.295\ min^{-1}$.

From Eq. (6), the time necessary to reach the complete wetting ($\theta = 0^{\circ}$) is estimated to be about 13.3 min for additive YN2 at 1850 °C, this is a interesting time to application in liquid phase sintering. Experiments made with additives YN1 and YN3 at similar conditions lead to a large dispersion of θ versus t. This result was also attributed to the coexistence of liquid and solid phases in the additive drops for temperatures close to 1850 °C. In order to get analogous behaviour of θ versus t for additives YN1 and YN3, the experiments should be conducted at temperatures $T \geq T_m$ (Table 2), since at these temperatures the drops are composed only of liquid.

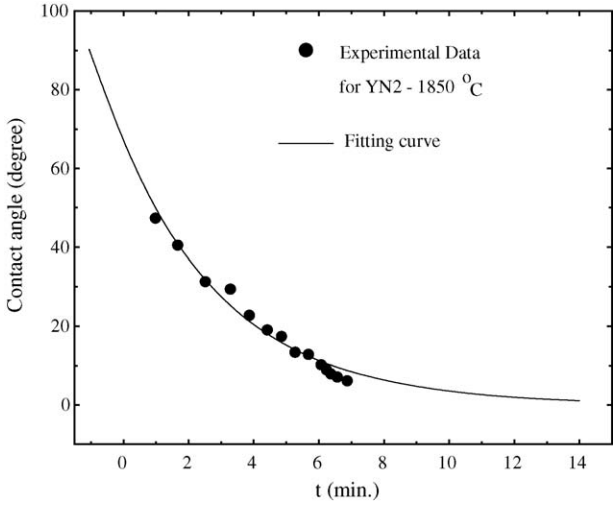

Fig. 6. Contact angle (θ) vs. time (t) curve of additive YN2 at 1850 °C on SiC plates.

4. Conclusion

Wettability tests of additives Y_2O_3/AlN on SiC substrate were conducted for three additives compositions. These compositions were at the eutectic point (YN2), at the left of the eutectic point (YN1) and at the right side of the eutectic point (YN3). YN1 and YN3 additives have a strong (exponential) decrease of θ versus T. However, they do not reach a complete wetting ($\theta = 0^{\circ}$), because the presence of solid phases in the drop accelerates θ versus T decay that spoils the dissolution. In this case there is probably the competition between the additive spreading and dissolution. The presence of solid phases in the additives drops YN1 and YN3 causes the decrease of the surfaces energies γ^{LV} and γ^{SL} and as a result a strong decrease of θ versus T. YN2 additive has a smooth decrease (quadratic) of θ versus T. The contact of the solid occurs with a large quantity of liquid, since the onset of the experiment. Then, a good dissolution is achieved and a complete wettability can be reached. Additive YN2 reaches complete wettability ($\theta_{min} = 0^{\circ}$) for $T \cong 1920\,^{\circ}C$. Despite those additives YN1 and YN3 do not reach complete wettability, they have $\theta_{min} \cong 6^{\circ}$ that is a pretty small value. Hence, additives YN1 and YN3, also have a good wettability. The present work showed that producing SiC ceramic using Y_2O_3/AlN (eutectic composition) like additive is very promising, because the complete wettability reached in a short period of time, so it is the driving force to the liquid phase sintering.

Acknowledgements

The authors acknowledge Fundação de Amparo à Pesquisa do Estado de São Paulo (FAPESP) (Grants 01/10664-6 and 01/11339-1), Conselho Nacional de Desenvolvimento Científico e Tecnológico (CNPq) and Coordenação de Aperfeiçoamento de Pessoal de Nível Superior (CAPES) for financial support.

References

1. Izhevskyi, V. A., Gênova, L. A., Bressiani, J. C. and Bressiani, A. H. A., Review article: silicon carbide. Structure, properties and processing. *Cerâmica*, 2000, **46**(297), 4–14.

2. Misra, A. K., Thermochemical analysis of the silicon carbide-alumina reaction with reference to liquid-phase sintering of silicon carbide. *J. Am. Ceram. Soc.*, 1991, **74**(2), 345–351.
3. Izhevskyi, V. A., Genova, L. A., Bressiani, A. H. A. and Bressiani, J. C., Liquid phase sintered SiC. Processing and transformation controlled microstructure tailoring. *Mater. Res.*, 2000, **3**, 131–138.
4. Esposito, L., Bellosi, A. and Landi, S. J., Interfacial forces in Si_3N_4-and SiC-based systems and their influence on the joining process. *J. Am. Ceram. Soc.*, 1999, **82**, 3597.
5. She, J. H. and Ueno, K., Effect of additive content on liquid-phase sintering on silicon carbide ceramics. *Mater. Res. Bull.*, 1999, **34**(10–11), 1629–1636.
6. Busker, G., Chroneos, A. and Grimes, R. W. J., Solution mechanisms for dopant oxides in yttria. *J. Am. Ceram. Soc.*, 1999, **82**(6), 1853.
7. Siddiqi, N., Bhoi, B., Paramguru, R. K., Sahajwalla, V. and Ostrovski, O., Slag-graphite wettabilitity and reaction kinetics Part 2 Wettability influenced by reduction kinetics. *Ironmak. Steelmak.*, 2000, **27**(6), 437–441.
8. Hadian, A. M. and Drew, R. A. L., Thermodynamic modelling of wetting silicon nitride/Ni-Cr-Si alloy interfaces. *Mater. Sci. Eng.*, 1994, **A189**, 209–217.
9. Chidambaram, P. R., Edwards, G. R. and Olson, D. L., A thermodynamic criterion to predict wettability at metal-alumina interfaces. *Metall. Trans.*, 1992, **23B**, 215–222.
10. Nicolopoulos, P., Agathopolos, S. G., Angelopoulos, N., Naoumidis, A. and Grubmeier, H., Wettability and interfacial energies in SiC-liquid metal systems. *J. Mater. Sci.*, 1992, **27**, 139–145.
11. Ureña, A., Escalera, M. D., Rodrigo, P., Baldonedo, J. L. and Gil, L., Active coating for SiC particles to reduce the degradation by liquid aluminium during processing of aluminium matrix composites: study of interfacial reactions. *J. Microsc.*, 2001, **201**(Pt 2), 122.
12. Chen, J., Wei, P., Mei, Q. and Huang, Y., The wettability of Y—Al—Si—O—N oxide glasses and its application in silicon nitride joining. *J. Eur. Ceram. Soc.*, 2000, **20**, 2685–2689.
13. Motta, F. V., Balestra, R. M., Ribeiro, S. and Taguchi, S. P., Wetting behaviour of SiC ceramics: Part I – E_2O_3/Al_2O_3 additive system. *Mater. Lett.*, 2004, **58**, 2805–2809.
14. Taguchi, S. P., Motta, F. V., Balestra, R. M. and Ribeiro, S., Wetting behaviour of SiC ceramics: Part II – Y_2O_3/Al_2O_3 and Sm_2O_3/Al_2O_3. *Mater. Lett.*, 2004, **58**, 2810–2814.
15. Lee, H. L., Nam, S. W., Rahn, B. S., Park, B. H. and Ran, D., Joining of silicon carbide using MgO—Al_2O_3—SiO_2 filler. *J. Mater. Sci.*, 1998, **33**, 5007–5014.
16. Siddiqi, N., Bhoi, B., Paramguru, R. K., Sahajwalla, V. and Ostrovski, O., Slag-graphite wettability and reaction kinetics. Part 1: Kinetics and mechanism of molten FeO reaction. *Ironmak. Steelmak.*, 2000, **27**(5), 367.
17. Eustathopoulos, N., Sobczak, N., Passerone, A. and Nogi, K., Measurement of contact angle and work of adhesion at high temperature. *J. Mater. Sci.*, 2005, **40**, 2271–2280.
18. Saiz, E., Cannon, R. M. and Tomsia, P., Reactive spreading: adsorption, ridgind and compound formation. *Acta Mater.*, 2000, 4449–4462.
19. Nowok, J. W., Mass transport phenomena at the liquid metal/substrate (metal, carbide) interface. *Mater. Sci. Eng.*, 1997, **A232**, 157.